Supplementary Materials

Sb(III) Removal from Aqueous Solutions by the Mesoporous Fe_3O_4/GO Nanocomposites: Modeling and Optimization Using Artificial Intelligence

X. L. Wu[1], R. S. Cao[1], J. W. Hu[1, 2 *], C. Zhou[1], and X. H. Wei[3]

[1] *Guizhou Provincial Key Laboratory for Information Systems of Mountainous Areas and Protection of Ecological Environment, Guizhou Normal University, Guiyang, Guizhou 550001, China*
[2] *Cultivation Base of Guizhou National Key Laboratory of Mountainous Karst Eco-environment, Institute of Karst, Guizhou Normal University, Guiyang, Guizhou 550001, China*
[3] *Department of Applied Chemistry, College of Chemistry and Molecular Engineering, Peking University, Beijing 100871, China*

Text S1. Adsorption equilibrium study

The Langmuir model was applied to describe the saturated monolayer adsorption, which can be represented as the following nonlinear (Eq. S1) and linear (Eq. S2) expressions (Yoon et al., 2016):

$$q_e = \frac{q_m k_L c_e}{1 + k_L c_e} \tag{1}$$

$$\frac{C_e}{q_e} = \frac{1}{k_L q_m} + \frac{C_e}{q_m} \tag{2}$$

where C_e is the equilibrium concentration of Sb(III) in solution (mg/L); q_e is the amount of Sb(III) adsorbed (mg/g); q_m is q_e for a complete monolayer (maximum adsorption capacity) (mg/g) ; k_L is adsorption equilibrium constant (L/mg).

The effect of isotherm shape can be employed to evaluate if an adsorption system is ‘favorable’ or ‘unfavorable’ (Pandey et al., 2010). The equilibrium parameter of R_L for the Langmuir isotherm is defined by the following relationship (Eq. S3):

$$R_L = \frac{1}{1 + K_L C_0} \tag{3}$$

where R_L is a dimensionless separation factor; C_0 and K_L represent the initial Sb(III) concentration (mg/L) and the Langmuir constant (L/mg), respectively. The parameter R_L for the isotherm shape is shown in Table S2.

The Freundlich model, an empirical equation, was used to describe the multilayer adsorption. The nonlinear (Eq. S4) and linear expressions (Eq. S5) (Cao et al., 2017) are shown as follows and:

$$q_e = k_F (c_e)^{1/n} \tag{4}$$

$$Inq_e = Ink_F + \frac{1}{n} InC_e \quad (5)$$

where K_F and *1/n* are empirical constants, representing the adsorption capacity and adsorption
intensity, respectively.

Temkin isotherm was proposed based on the chemisorption of an adsorbate onto the adsorbent. Its computational equation (Cao et al., 2017) is described as follows (Eq. S6):

$$q_e = a + b \log C_e \quad (6)$$

where *a* and *b* are constants, which can be calculated by the slope and intercept of the linear plot. In addition, chi square test (x^2) (Boparai et al., 2011), the sum of absolute errors (SAE) (Cao et al., 2017) and average percentage errors (APE) (Boparai et al., 2011) were used to validate the credibility of three adsorption isotherms models. Their equations are shown below:

$$SAE = \sum_{i=1}^{n} \left| q_{e,\exp} - q_{e,cal} \right|_i \quad (7)$$

$$x^2 = \sum_{i=1}^{n} \left| \frac{\left(q_{e,exp} - q_{e,cal} \right)^2}{q_{e,cal}} \right|_i \quad (8)$$

$$APE(\%) = \frac{100}{N} \times \sum_{i=1}^{n} \left| \frac{q_{e,cal} - q_{e,exp}}{q_{e,cal}} \right|_i \quad (9)$$

where $q_{e,exp}$ and $q_{e,cal}$ represent the experimental and calculated adsorption capacity (mg/g), respectively; *N* is the number of experiments.

Table S1. Level of operating parameters in Box-Behnken experimental design

Sample	Parameters	Maximum	Middle	Minimum
A	Contact Time (min)	70 (+1)	60 (0)	50 (-1)
B	Initial Sb(III) concentration ($mg \cdot L^{-1}$)	70 (+1)	50 (0)	30 (-1)
C	Temperature (◦C)	30 (+1)	25 (0)	20 (-1)
D	Initial pH	9 (+1)	7 (0)	5 (-1)

Table S2. The parameter R_L for the isotherm shape

Value of R_L	Type of Isotherm
$R_L > 1$	unfavorable
$R_L = 1$	linear
$0 < R_L < 1$	favorable
$R_L = 0$	irreversible

Table S3. Size distribution calculated from SEM image of Fe_3O_4/GO nanocomposites

Distridution/nm	Mean/nm	Amount	Frequency
13-17.5	15.25	1	1.00%
17.5-22	19.75	21	21.00%
22-26.5	24.25	16	16.00%
26.5-31	28.75	23	23.00%
31-35.5	33.25	12	12.00%
35.5-40	37.75	11	11.00%
40-44.5	42.25	9	9.00%
44.5-49	46.75	5	5.00%
49-53.5	51.25	1	1.00%
53.5-58	55.75	1	1.00%

Table S4. Experimental design matrix and results

Sample	Initial pH	Contact time (min)	Temperature (℃)	Initial Sb(III) concentration (mg/L)	Experimental value (%)	Predicted value (%)	Absolute error (%)
1	7	70	30	50	83.13	86.18	3.05
2	7	60	25	50	82.79	81.51	1.28
3	7	60	25	50	85.54	81.51	4.03
4	7	60	20	70	81.27	76.84	4.43
5	9	60	20	50	80.1	75.02	5.08
6	7	50	20	50	82.86	83.79	0.93
7	7	70	25	30	88.68	86.49	2.19
8	7	70	25	70	78.01	77.01	1
9	9	50	25	50	75.9	76.29	0.39
10	7	60	30	70	80.12	73.9	6.22
11	7	60	25	50	79.2	81.51	2.31
12	7	70	20	50	71.95	76.6	4.65
13	9	60	25	30	74.02	77.15	3.13
14	5	50	25	50	59.99	60.96	0.97
15	5	60	30	50	58.44	61.11	2.67

16	9	60	25	70	69.95	78.36	8.41
17	7	50	30	50	70.48	69.81	0.67
18	9	70	25	50	79.8	77.25	2.55
19	5	60	20	50	68.37	67.64	0.73
20	7	60	20	30	78.24	82.89	4.65
21	5	60	25	70	52.57	56.04	3.47
22	7	60	25	50	80.93	81.51	0.58
23	9	60	30	50	78.83	77.15	1.68
24	5	70	25	50	71.14	69.18	1.96
25	7	60	30	30	78.58	81.43	2.85
26	5	60	25	30	77.87	73.44	4.43
27	7	50	25	30	80.62	79.21	1.41
28	7	60	25	50	79.1	81.55	2.45
29	7	50	25	70	75.34	75.12	0.22

Table S5. Weights and biases input-layers (w_i and b_i) and hidden-layers (w_j and b_j)

	w_i				b_i	w_j	b_j
	Input weight						
	Contact time	pH	Initial concentration	Temperature			
1	-1.8834	1.1151	-0.0802	1.1836	-2.4896	-0.8571	0.2980
2	-0.0413	0.8787	1.6538	-1.6398	1.9363	0.0433	
3	-1.4136	1.7186	0.4677	-1.0137	1.3831	-0.8065	
4	1.8325	1.4966	0.4505	-0.6303	0.8299	0.6363	
5	1.0941	-0.8531	1.8489	0.9245	-0.2766	0.6351	
6	0.0023	0.9613	1.4776	-1.7580	-0.2766	0.4449	
7	-0.1877	-1.9623	0.4982	1.4366	0.8299	-0.7003	
8	-1.3399	-1.4284	-0.9648	-1.1965	-1.3831	0.3192	
9	1.0563	1.4167	-1.5096	0.8925	1.9363	0.0372	
10	-1.9018	0.0001	1.6065	-0.0242	-2.4896	0.9459	

Table S6. The values of R_L for the adsorption of Sb(III) by the Fe_3O_4/GO nanocomposites

Initial concentration (mg/L)	R_L value
1	0.5659
2	0.3946
5	0.2068
10	0.1153
20	0.0612
30	0.0416
40	0.0316
50	0.0254

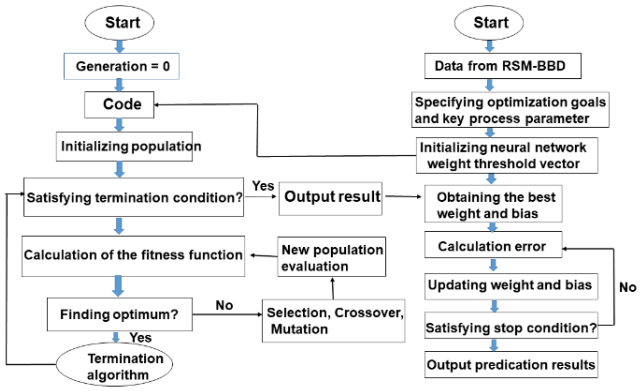

Figure S1. The flow chart of ANN-GA optimization process.

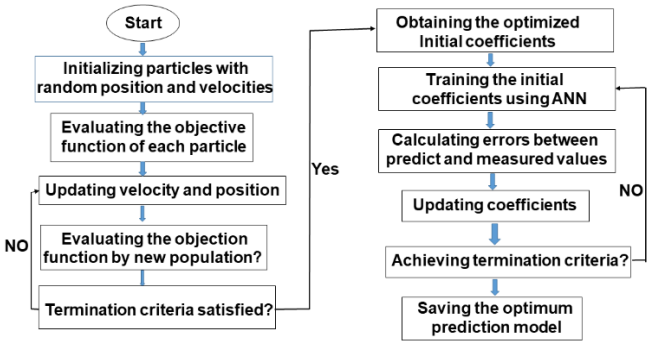

Figure S2. The flow chart of ANN-PSO optimization process.

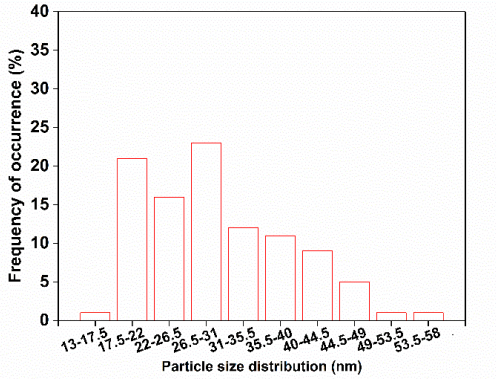

Figure S3. Size distributions of Fe_3O_4.

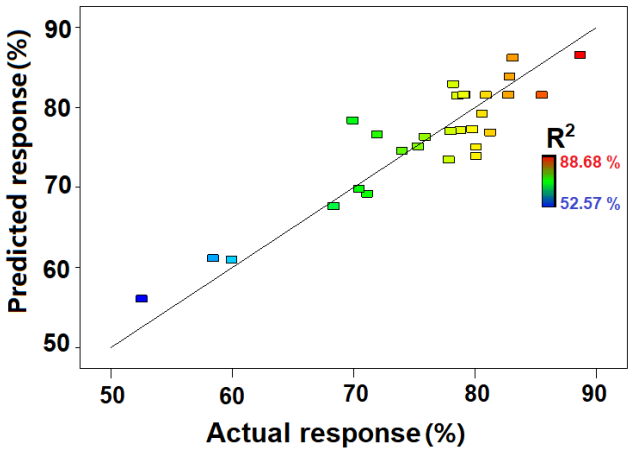

Figure S4. The experimental and predictive values of the responses

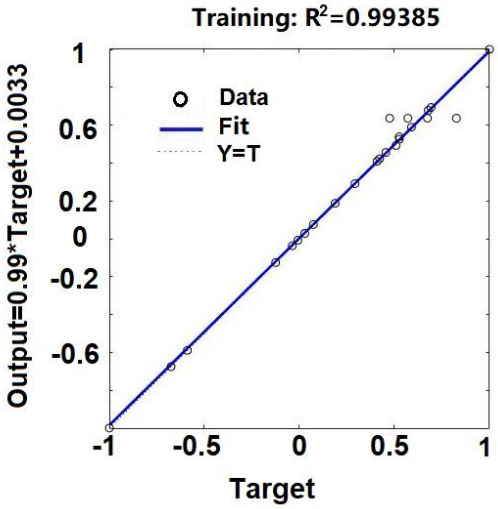

Figure S5. The experimental data versus the predicted data of normalized removal.

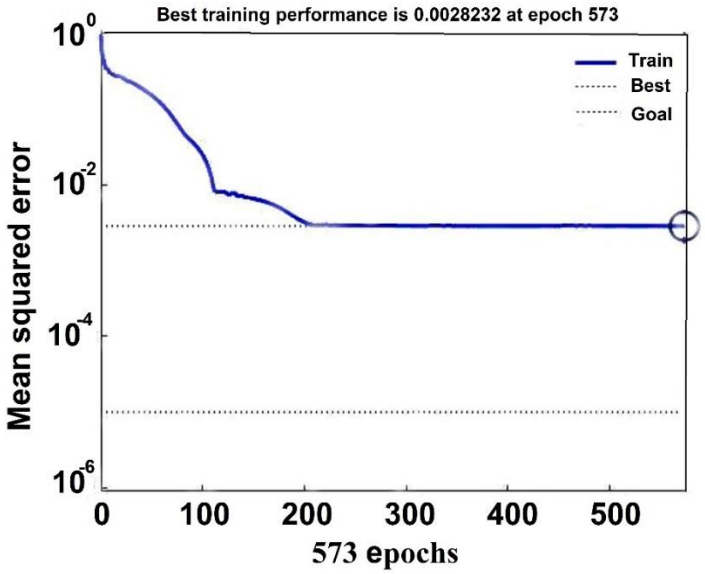

Figure S6. The relationship between MSE and the number of epochs.

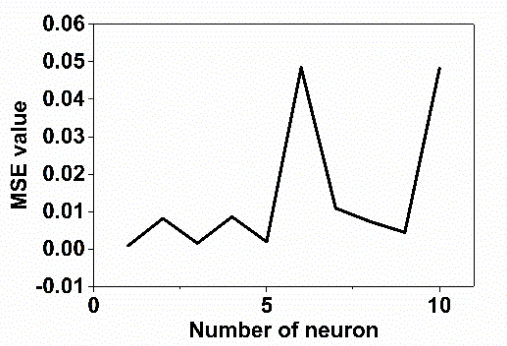

Figure S7. The number of neurons in hidden layer.

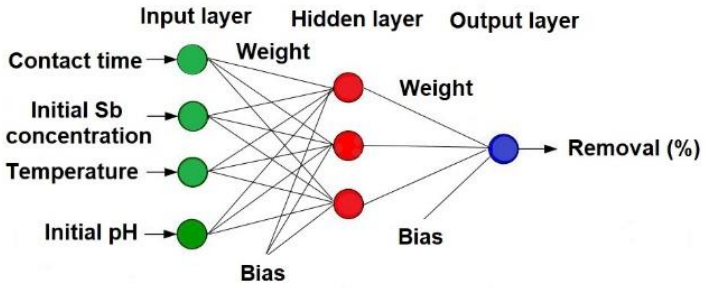

Figure S8. Structure of a back-propagation artificial neural network.

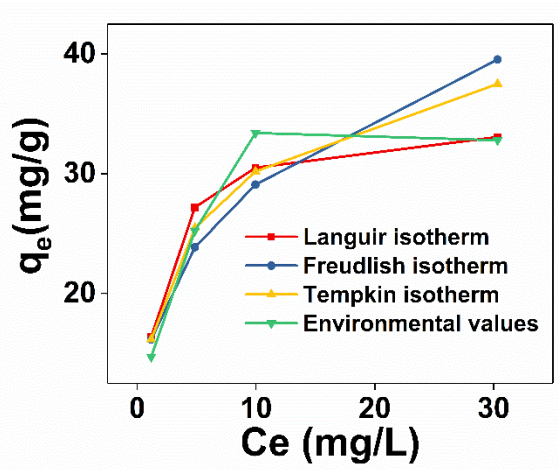

Figure S9. Adsorption isotherm for Sb(III) onto Fe_3O_4/GO nanocomposites (Fe_3O_4/GO dosage = 30 mg; initial pH = 7.0; contact time = 60 min; temperature = 25 ℃).

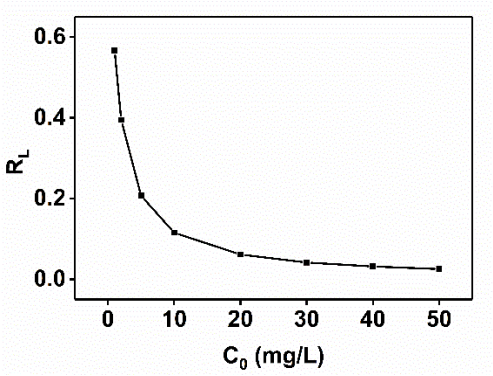

Figure S10. Plot of separation factor versus initial Sb(III) concentration.

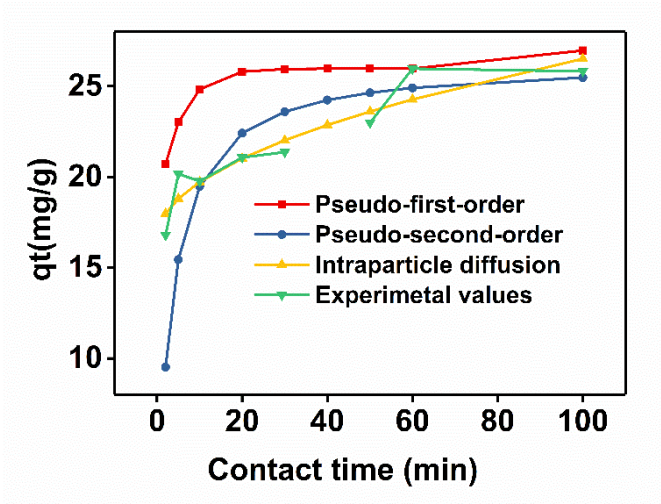

Figure S11. Time dependent study of Sb (III) removal by Fe_3O_4/GO nanocomposites (Fe_3O_4/GO dosage = 30 mg; initial Sb(III) concentration = 20 mg/L; temperature = 25 ℃; initial pH = 7.0).

References

Boparai, H. K., Joseph, M., and O'Carroll, D. M. (2011). Kinetics and thermodynamics of cadmium ion removal by adsorption onto nano zerovalent iron particles. *J. Hazard. Mater.*, 186, 458-465, doi:10.1016/j.jhazmat.2010.11.029.

Cao, R. S, Fan, M. Y., Hu, J. W., Ruan, W. Q., Xiong, K. N., and Wei, X. H., (2017). Optimizing low-concentration mercury removal from aqueous solutions by reduced graphene oxide-supported Fe_3O_4 composites with the aid of an artificial neural network and genetic algorithm. *Materials*, 10, 1279-1283, doi:10.3390/ma10111279.

Pandey, P. K., Sharma, S. K., and Sambi S. S. (2010). Kinetics and equilibrium study of chromium adsorption on zeoliteNaX. *Inter. J. Environ. Sci. Te.*, 7, 395-404, doi:10.1007/BF03326149.

Yoon, Y. J, Park, W. K., Hwang, T. M., Yoon, D. H., Yang, W. S., and Kang, J. W. (2016). Comparative evaluation of magnetite–graphene oxide and magnetite-reduced graphene oxide composite for As(III) and As(V) removal. *J. Hazard. Mater.*, 304, 196-204, doi:10.1016/j.jhazmat.2015.10.053.